4 Continuum elastic or viscoelastic models for the cell

Mohammad R. K. Mofrad, Helene Karcher, and Roger D. Kamm

ABSTRACT: Cells can be modeled as continuum media if the smallest operative length scale of interest is much larger than the distance over which cellular structure or properties may vary. Continuum description uses a coarse-graining approach that replaces the contributions of the cytoskeleton's discrete stress fibers to the local microscopic stress-strain relationship with averaged constitutive laws that apply at macroscopic scale. This in turn leads to continuous stress-strain relationships and deformation descriptions that are applicable to the whole cell or cellular compartments. Depending on the dynamic time scale of interest, such continuum description can be elastic or viscoelastic with appropriate complexity. This chapter presents the elastic and viscoelastic continuum multicompartment descriptions of the cell and shows a successful representation of such an approach by implementing finite element-based two- and three-dimensional models of the cell comprising separate compartments for cellular membrane and actin cortex, cytoskeleton, and nucleus. To the extent that such continuum models can capture stress and strain patterns within the cell, it can help relate biological influences of various types of force application and dynamics under different geometrical configurations of the cell.

Introduction

Cells can be modeled as continuum media if the smallest length scale of interest is significantly larger than the dimensions of the microstructure. For example when whole-cell deformations are considered, the length scale of interest is at least one or two orders of magnitude larger than the distance between the cell's microstructural elements (namely, the cytoskeletal filaments), and as such a continuum description may be appropriate. In the case of erythrocytes or neutrophils in micropipette aspiration, the macroscopic mechanical behavior has been successfully captured by continuum viscoelastic models. Another example is the cell deformation in magnetocytometry, the application of a controlled force or torque via magnetic microbeads tethered to a single cell. Because the bead size and the resulting deformation in such experiments are much larger than the mesh size of the cytoskeletal network, a continuum viscoelastic model has been successfully applied without the need to worry about the heterogeneous distribution of filamentous proteins in the cytoskeleton. It should be noted that in using a continuum model, there are no constraints in terms of isotropy or homogeneity of properties, as these can easily be incorporated to the extent they are

known. Predictions of the continuum model, however, are only as good as the constitutive law – stress-strain relation – on which they are based. This could range from a simple linear elasticity model to a description that captures the viscoelastic behavior of a soft glassy material (see, for example Chapter 3). Accordingly, the continuum model tells us nothing about the microstructure, other than what might be indirectly inferred based on the ability of one constitutive law or another to capture the observed cellular strains. It is important that modelers recognize this limitation.

In essence, continuum mechanics is a coarse-graining approach that replaces the contributions of the cytoskeleton's discrete stress fibers to the local microscopic stress-strain relationship with averaged constitutive laws that apply at macroscopic scale. This in turn leads to continuous stress-strain relationships and deformation descriptions that are applicable to the whole cell or cellular compartments. Depending on the dynamic time scale of interest, such continuum descriptions can be elastic or viscoelastic with appropriate complexity.

This chapter presents elastic and viscoelastic continuum multicompartment descriptions of the cell and shows a successful representation of such approaches by implementing finite element-based two- and three-dimensional models of the cell comprising separate compartments for cellular membrane and actin cortex, cytoskeleton, and the nucleus. To the extent that such continuum models can capture stress and strain patterns within the cell, they can help us relate biological influences of various types of force application and dynamics under different geometrical configurations of the cell.

By contrasting the computational results against experimental data obtained using various techniques probing single cells – such as micropipette aspiration (Discher et al., 1998; Drury and Dembo, 2001), microindentation (Bathe et al., 2002), atomic force microscopy (AFM) (Charras et al., 2001), or magnetocytometry (Figs. 4-7, 4-8, Karcher et al., 2003; Mack et al., 2004) – the validity and limits of such continuum mechanics models will be assessed. In addition, different aspects of the model will be characterized by examining, for instance, the mechanical role of the membrane and actin cortex in the overall cell behavior. Lastly, the applicability of different elastic and viscoelastic models in the form of various constitutive laws to describe the cell under different loading conditions will be addressed.

Purpose of continuum models

Continuum models of the cell are developed toward two main purposes: analyzing experiments probing single cell mechanics, and evaluating the level of forces sensed by various parts of the cell *in vivo* or *in vitro*. In the latter case, a continuum model evaluates the stress and strain patterns induced in the cell by the experimental technique. Comparison of theoretical and computational predictions proposed by the continuum model against the experimental observations then allows for deduction of the cell's mechanical properties. In magnetocytometry, for example, the same torque or tangential force applied experimentally to a microbead attached atop a cell is imposed in continuum models of the cell. Material properties introduced in the model that reproduce the observed bead displacement yield possible mechanical properties of the probed cell (see Mijailovich et al., 2002, and Fig. 4-7 for torque application,
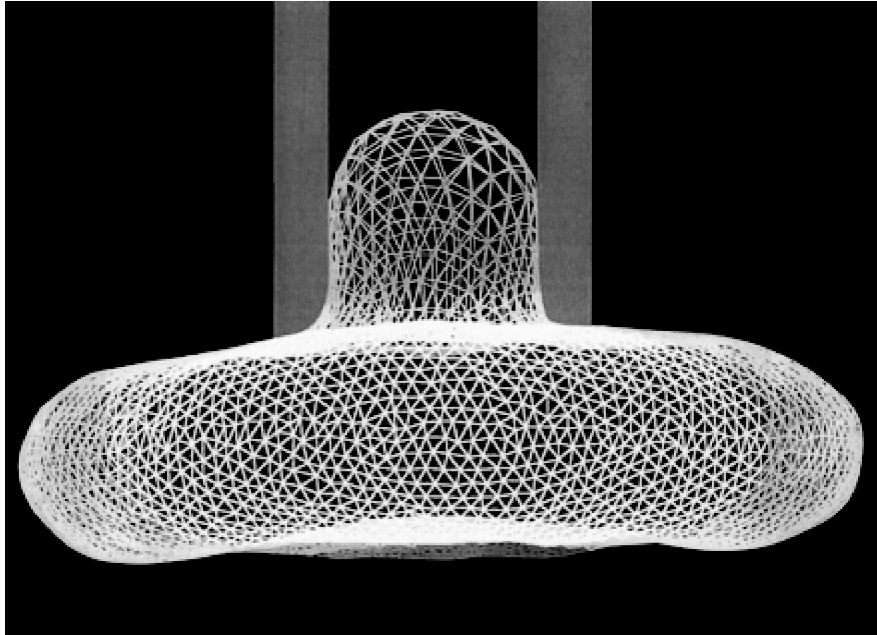
Fig. 4-1. Simulation of a small erythrocyte under aspiration. The micropipette, indicated by the solid gray shading, has an inside diameter of 0.9 μm. The surface of the cell is triangulated with 6110 vertex nodes that represent the spectrin-actin junction complexes of the erythrocyte cytoskeleton. The volume of the cell is 0.6 times the fully inflated volume, and the simulation is drawn from the stress-free model in the free shape ensemble. From Discher et al., 1998.

and Karcher et al., 2003, and Fig. 4-8 for tangential force application). Continuum models have also shed light on mechanical effects of other techniques probing single cells, such as micropipette aspiration (Figs. 4-1, 4-6, and for example, Theret et al., 1988; Yeung and Evans, 1989; Dong and Skalak, 1992; Sato et al., 1996; Guilak et al., 2000; Drury and Dembo, 2001), microindentation (for example, Bathe et al., 2002, probing neutrophils, Fig. 4-2 left), atomic force microscopy (AFM) (for example, Charras et al., 2001 and Charras and Horton, 2002, deducing mechanical
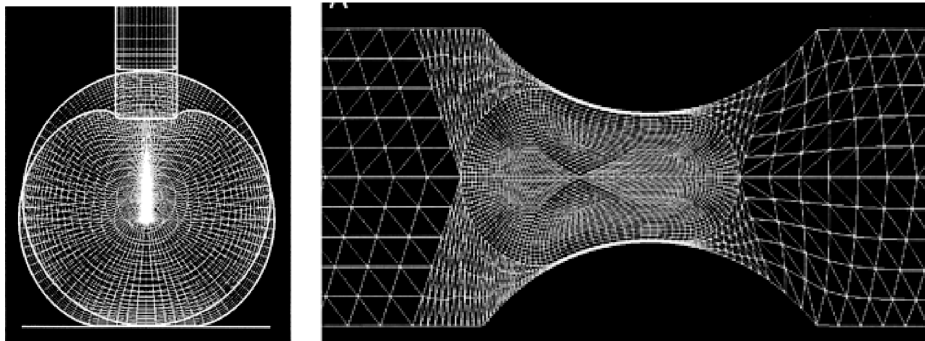
Fig. 4-2. Microindentation of a neutrophil (left) and passage through a capillary (right) (finite element model). From Bathe et al., 2002.
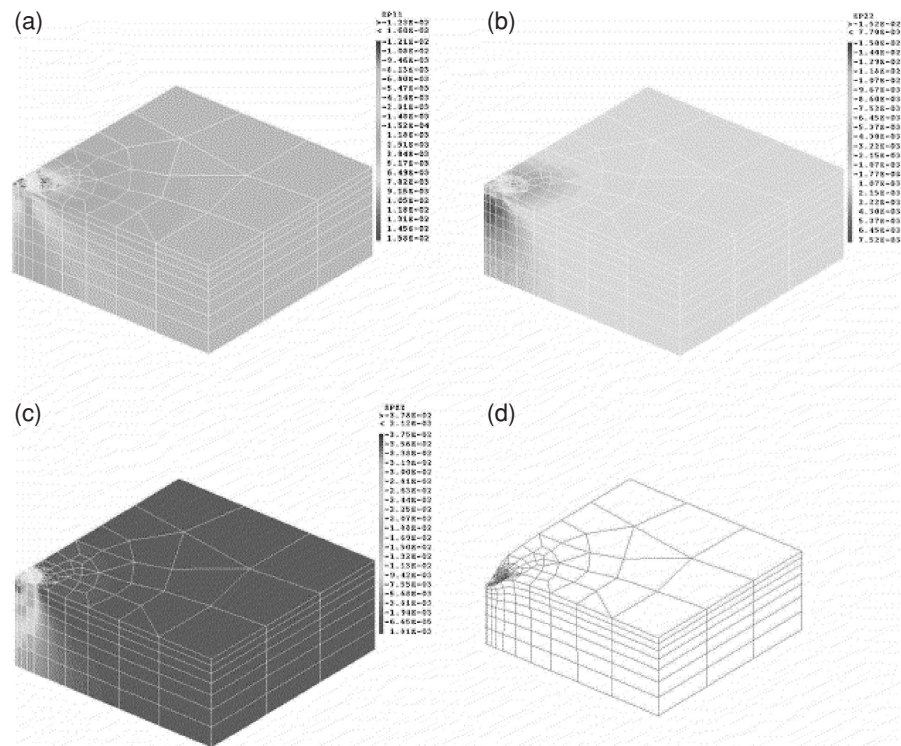
Fig. 4-3. Strain distributions elicited by AFM indentation. All of the scales are in strains. The numerical values chosen for this simulation were: $E = 10$ kPa, $\nu = 0.3$, $R = 15$ μm, $F = 1$ nN. (a) Radial strain distribution. The largest radial strains are found on the cell surface. A large strain gradient is present at the boundary between the region where the sphere is in contact with the cell surface and the region where it is not. (b) Tangential strain distribution. The largest tangential strains occurred at the cell surface in the area of indentation. (c) Vertical strain distribution. The largest vertical strains were located directly under the area of indentation within the cell thickness. (d) Deformations elicited by AFM indentation. The deformations have been amplified 15-fold in the z-direction. From Charras et al., 2001.

properties of osteoblasts, Figs. 4-3, 4-4), magnetocytometry (Figs. 4-7, 4-8, Karcher et al., 2003; Mack et al., 2004; Mijailovich et al., 2002), or optical tweezers (for example, Mills et al., 2004 stretching erythrocytes, Fig. 4-5). Finally, comparison of continuum models with corresponding experiments could help to distinguish active biological responses of the cell (such as remodeling and formation of pseudopods) from passive mechanical deformations, the only deformations captured by the model. This capability has not been exploited yet to the best of our knowledge.

In addition to helping interpret experiments, continuum models are also used to evaluate strains and stresses under biological conditions (for example, Fung and Liu, 1993, for endothelium of blood vessels). One example is found in the microcirculation where studies have examined the passage of blood cells through a narrow capillary (for example, Bathe et al., 2002, for neutrophils (Fig. 4-2 left), Barthes-Biesel, 1996, for erythrocytes) where finite element models have been used to predict the changes in cell shape and the cell's transit time through capillaries. In the case
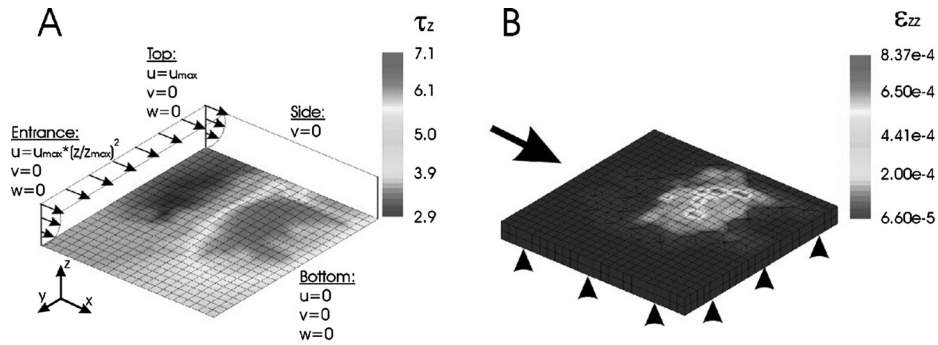
Fig. 4-4. The effect of fluid shear. (*a*) The shear stress resultant in the *z*-direction (τ_z) for a nominal 5 Pa shear stress on a flat substrate. The shear stresses are tensile and lower upstream and higher downstream. The imposed parabolic flow profile is shown at the entry and the boundary conditions are indicated on the graph. (*b*) The vertical strain distribution (ε_{zz}) for a cell submitted to fluid shear stresses. Black triangles indicate where the substrate was fully constrained. The cellular strains are maximal downstream from the cell apex and in the cellular region. In (*a*) and (*b*), the arrow indicates the direction of flow. From Charras and Horton, 2002.

of neutrophils, these inputs are crucial in understanding their high concentration in capillaries, neutrophil margination, and in understanding individual neutrophil activation preceding their leaving the blood circulation to reach infection sites. Neutrophil concentration depends indeed on transit time, and activation has recently been shown experimentally to depend on the time scale of shape changes (Yap and Kamm, 2005). Similarly, continuum models can shed light on blood cells' dysfunctional microrheology arising from changes in cell shape or mechanical properties (for example, time-dependent stiffening of erythrocytes infected by malaria parasites in Mills et al., 2004 (Fig. 4-5)).

Other examples include the prediction of forces exerted on a migrating cell in a three-dimensional scaffold gel (Zaman et al., 2005), prediction of single cell attachment and motility on a substrate, for example the model for fibroblasts or the unicellular organism Ameboid (Gracheva and Othmer, 2004), or individual protopod dynamics based on actin polymerization (Schmid-Schönbein, 1984).

Principles of continuum models

A continuum cell model provides the displacement, strain, and stress fields induced in the cell, given its initial geometry and material properties, and the boundary conditions it is subjected to (such as displacements or forces applied on the cell surface). Laws of continuum mechanics are used to solve for the distribution of mechanical stress and deformation in the cell. Continuum cell models of interest lead to equations that are generally not tractable analytically. In practice, the solution is often obtained numerically via discretization of the cell volume into smaller computational cells using (for example) finite element techniques.

A typical continuum model relies on linear momentum conservation (applicable to the whole cell volume). Because body forces within the cell are typically small, and,

maximum principal strain

0% 20% 40% 60% 80% 100% 120%

experiment   simulations

0 pN

67 pN

130 pN

193 pN

(a)   (b)   (c)
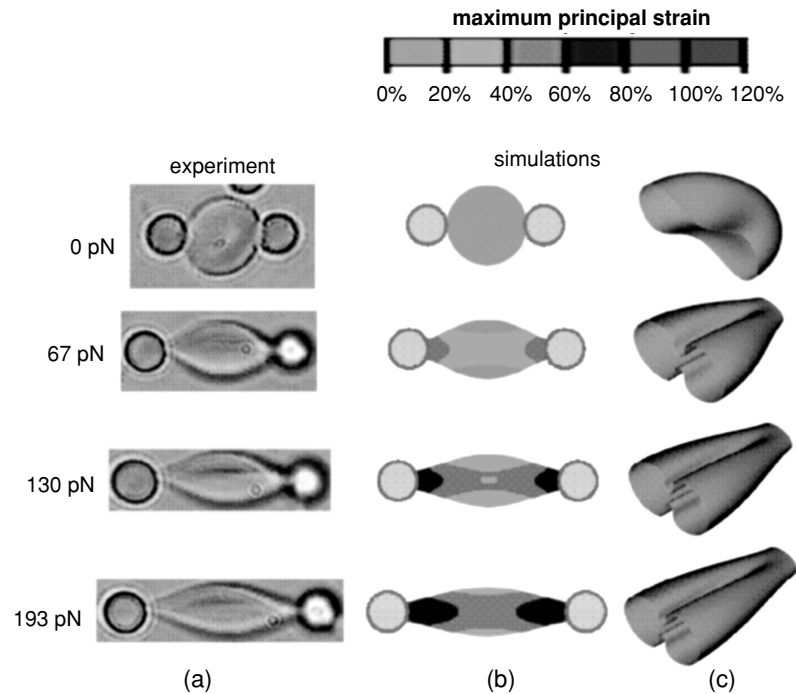
Fig. 4-5. Images of erythrocytes being stretched using optical tweezer at various pulling forces. The images in the left column are obtained from experimental video photography whereas the images in the center column (top view) and in the right column (half model 3D view) correspond to large deformation computational simulation of the biconcave red cell. The middle column shows a plan view of the stretched biconcave cell undergoing large deformation at the forces indicated on the left. The predicted shape changes are in reasonable agreement with observations. The contours in the middle column represent spatial variation of constant maximum principal strain. The right column shows one half of the full 3D shape of the cell at different imposed forces. Here, the membrane is assumed to contain a fluid with preserved the internal volume. From Mills et al., 2004.

at the scale of a cell, inertial effects are negligible in comparison to stress magnitudes the conservation equation simply reads:

$$\nabla \cdot \underline{\underline{\sigma}} = \underline{0}$$

with $\underline{\underline{\sigma}}$ = Cauchy's stress tensor.

Boundary conditions

For the solution to uniquely exist, either a surface force or a displacement (possibly equal to zero) should be imposed on each point of the cell boundary. Continuity of normal surface forces and of displacement imposes necessary conditions to ensure uniqueness of the solution.

Mechanical and material characteristics

Mechanical properties of the cell must be introduced in the model to link strain and stress fields. Because a cell is composed of various parts with vastly different mechanical properties, the model ideally should distinguish between the main parts
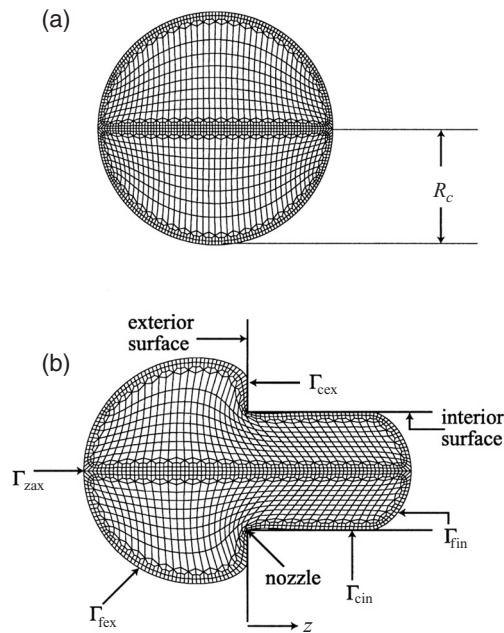
Fig. 4-6. Geometry of a typical computational domain at two stages. (*a*) The domain in its initial, round state. (*b*) The domain has been partially aspirated into the pipet. Here, the interior, exterior, and nozzle of the pipet are indicated. Γ_{fin}, free-interior; Γ_{fex}, free-exterior; Γ_{cin}, constrained-interior; and Γ_{cex}, constrained-exterior boundaries. There is a fifth, purely logical boundary, Γ_{zax}, which is the axis of symmetry. From Drury and Dembo, 2001.

of the cell, namely the plasma membrane, the nucleus, the cytoplasm, and organelles, which are all assigned different mechanical properties. This often leads to the introduction of many poorly known parameters. A compromise must then be found between the number of cellular compartments modeled and the number of parameters introduced.

The *cytoskeleton* is difficult to model, both because of its intricate structure and because it typically exhibits both solid- and fluid-like characteristics, both active and passive. Indeed, a purely solid passive model would not capture functions like crawling, spreading, extravasion, invasion, or division. Similarly, a purely fluid model would fail in describing the ability to maintain the structural integrity of cells, unless the membrane is sufficiently stiff.

The *nucleus* has generally been found to be stiffer and more viscous than the cytoskeleton. Probing isolated chondrocyte nuclei with micropipette aspiration Guilak et al. (2000) found nuclei to be three to four times stiffer and nearly twice as viscous as the cytoplasm. Its higher viscosity results in a slower time scale of response, so that the nucleus can often be considered as elastic, even when the rest of the cell requires viscoelastic modeling. Nonetheless, the available data on nuclear stiffness seem to be rather divergent, with values ranging from 18 Pa to nearly 10 kPa (Tseng et al., 2004; Dahl et al., 2005), due perhaps to factors such as differences in cell type, measurement technique, length scale of measurement, and also method of interpretation.

The *cellular membrane* has very different mechanical properties from the rest of the cell, and hence, despite its thinness, often requires separate modeling. It is more

(a) (b)

(c) (d)
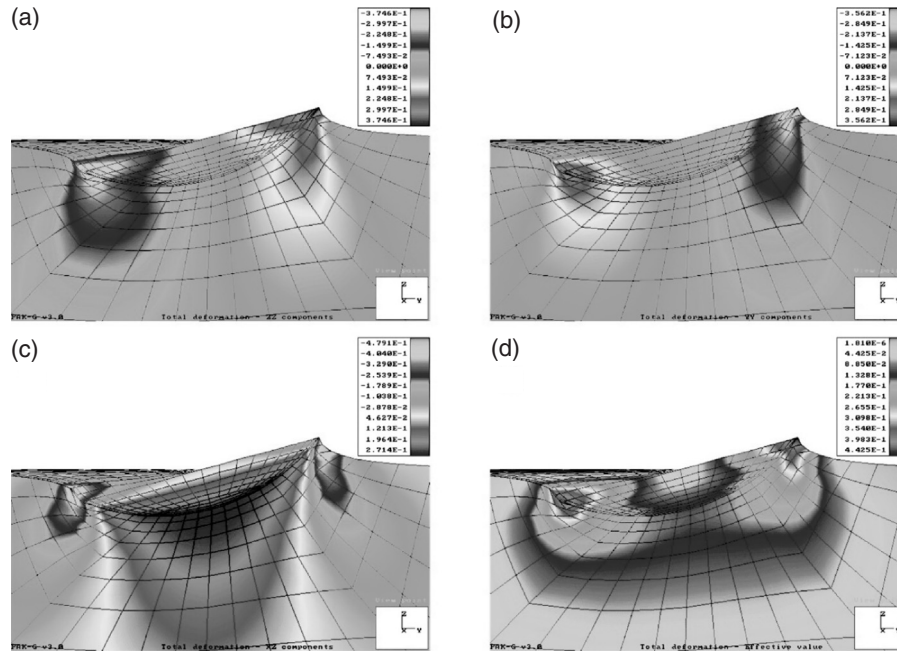
Fig. 4-7. Deformed shapes and strain fields in a cell 5 μm in height for bead embedded 10% of its diameter. Shown are strain fields of the components of strain: ε_{zz} (a), ε_{yy} (b), ε_{yz} (c), and the effective strain ε_{eff} (d). The effective strain is defined as: $\varepsilon_{eff} = \sqrt{\frac{2}{3}\varepsilon_{ij} - \varepsilon_{ij}}$, where ε_{ij} are strain components in Cartesian system x_i (x, y, z). From Mijailovitch et al., 2002.

fluid-like (Evans, 1989; Evans and Yeung, 1989) and should be modeled as a vis-coelastic material with time constants of the order of tens of μs.

The *cortex*, that is, the shell of cytoskeleton that is just beneath the membrane, is in most cell types stiffer than the rest of the cytoskeleton. Bending stiffness of the membrane and cortex has been measured in red blood cells (Hwang and Waugh, 1997; Zhelev et al., 1994). A cortical tension when the cell is at its (un-stimulated) resting state has also been observed in endothelial cells and leukocytes (Schmid-Schönbein et al., 1995).

Example of studied cell types

Blood cells: leukocytes and erythrocytes

Blood cells are subjected to intense mechanical stimulation from both blood flow and vessel walls, and their rheological properties are important to their effectiveness in per-forming their biological functions in the microcirculation. Modeling of neutrophils' viscoelastic large deformations in narrow capillaries or in micropipette experiments has shed light on their deformation and their passage time through a capillary or entrance time in a pipette. Examples of such studies are Dong et al. (1988), Dong and Skalak (1992), Bathe et al. (2002), and Drury and Dembo (2001) (see Fig. 4.6), who used finite element techniques and/or analytical methods to model the large de-formations in neutrophils. Shape recovery after micropipette aspiration – a measure
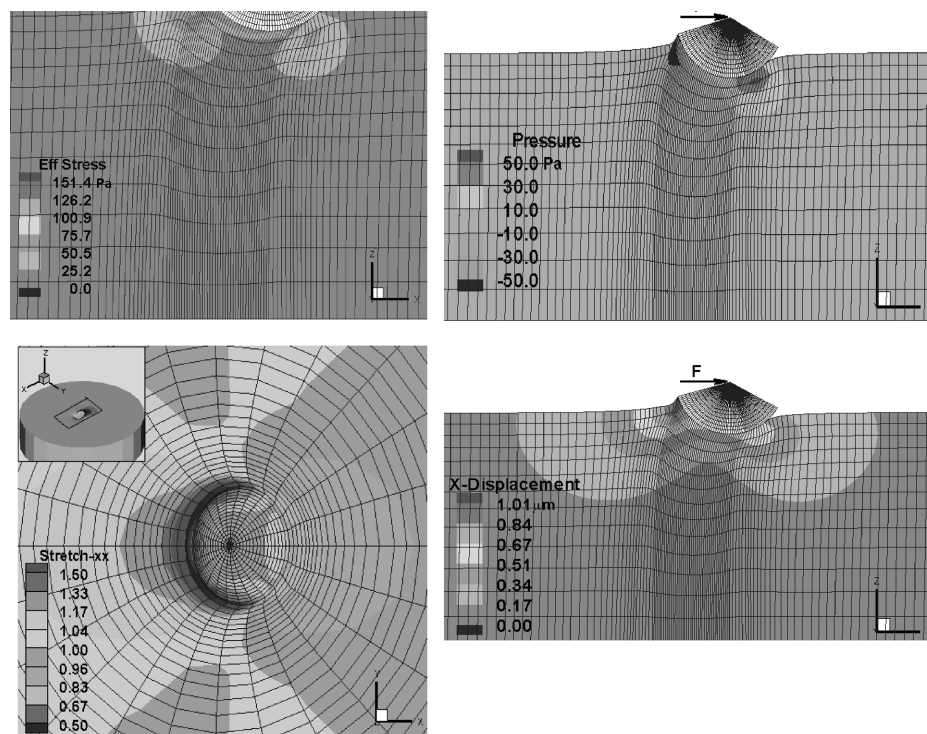
Fig. 4-8. Computational finite element models of a cell monolayer being pulled at 500 pN using magnetic cytometry experiment. Top panels show the pressure and effective stress fields induced in the cell after 2 s. (effective stress is a scalar invariant of the stress tensor excluding the compressive part). Lower left panel shows the membrane xx-stretch (in the direction of the applied force), while the lower right panel shows the induced deformation in the cytoskeleton in the direction of the applied force. From Karcher et al., 2003.

of the neutrophil's viscoelastic properties and its active remodeling – was for example investigated with a theoretical continuum model consisting of two compartments: a cytoplasm modeled as a Newtonian liquid, and a membrane modeled with a Maxwell viscoelastic fluid in the first time of recovery and a constant surface tension for the later times (Tran-Son-Tay et al., 1991). Erythrocytes have typically been modeled as viscoelastic membranes filled with viscous fluids, mostly to understand microcirculation phenomena, but also to explain the formation of "spikes" or crenations on their surface (Landman, 1984).

Adherent cells: fibrobasts, epithelial cells, and endothelial cells

Many types of cell, anchored to a basal substrate and sensitive to mechanical stimuli – like fibrobasts and epithelial and endothelial cells – have been probed by magnetocytometry, the forcing of a μm-sized bead attached atop a single cell through a certain type of membrane receptor (such as integrins).

Continuum modeling of this experiment was successfully developed to analyze the detailed strain/stress fields induced in the cell by various types of bead forcing (oscillatory or ramp forces of various magnitudes) (Mijailovitch et al., 2002; Fig. 4-7).
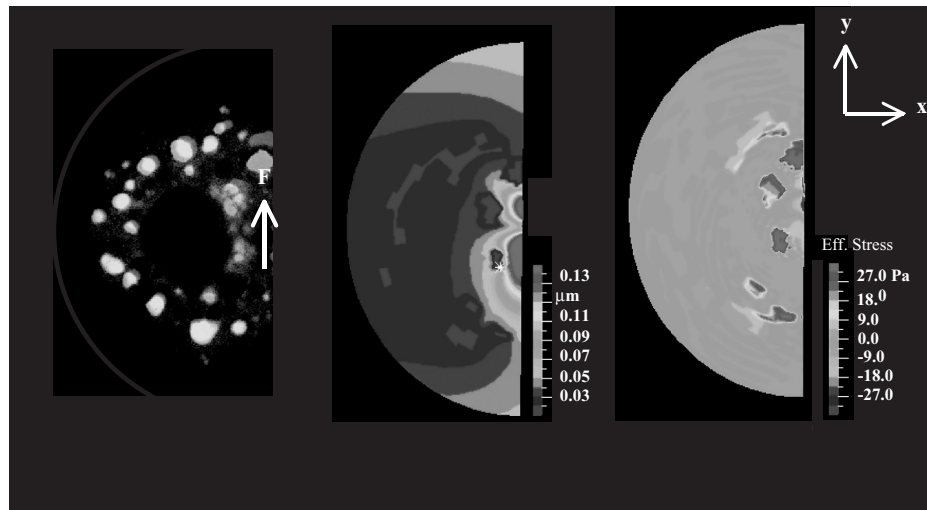
Fig. 4-9. A continuum, viscoelastic finite element simulation representing experimental cell contact sites on the basal cell surface estimated the focal adhesion shear stress distribution during magneto-cytometry. Left panel shows merged experimental fluorescent images depicting the focal adhesion sites. Middle and right panels show displacement and shear stress in the basal membrane of the cell. Zero displacement and elevated shear stresses are evident in the focal adhesion regions. From Mack et al., 2004.

(Karcher et al., 2003; Fig. 4-8). Modeling the cell with two Maxwell viscoelastic compartments representing, respectively, the cytoskeleton and the membrane/cortex, the authors found that the membrane/cortex contributed a negligible mechanical effect on the bead displacement at the time scales corresponding to magnetocytometry.

Comparison with experiments on NIH 3T3 fibroblasts led to a predicted viscoelastic time scale of ∼1 s and a shear modulus of ∼1000 Pa for these cells. In addition, the model showed that the degree to which the bead is embedded in the cell, a parameter difficult to control and measure in experiments (Laurent et al., 2002; Ohayon et al., 2004), dramatically changes the magnitude of stress and strain, although it influences their pattern very little. Continuum modeling also allowed for modulation of cell height and material properties to investigate the behavior of different adherent cell types. It also demonstrated that the response of the cell when forced with the microbead was consistent with that of a linear elastic model, quite surprising in view of the locally large strains.

The cell attachment to its substrate by the basal membrane was later modified to investigate force transmission from the bead to the basal membrane (Mack et al., 2004) (Fig. 4-9). Only experimentally observed points of attachments, that is, focal adhesion sites, were fixed in the model, allowing for the rest of the cell substrate to move freely. Forcing of the bead on the apical surface of NIH 3T3 fibroblasts preferentially displaced focal adhesion sites closer to the bead and induced a larger shear on the corresponding fixed locations in the model, implying that focal adhesion translation correlates with the local level of force they sense.

An alternative experiment to probe cell deformation and adhesion consists of plating them on a compliant substrate. Finite element modeling of cells probed by this

technique was recently used to evaluate the stress and strain experienced at the nuclear envelope, thereby investigating the mechanical interplay between the cytoskeleton and the nucleus. The ultimate goal of this study was to identify potential sources of mechanical dysfunction in fibroblasts deficient in specific structural nuclear membrane proteins (Hsiao, 2004). The model showed that the effect of nuclear shape, relative material properties of the nucleus and cytoskeleton, and focal adhesion size were important parameters in determining the magnitude of stress and strain at the nucleus/cytoskeleton interface.

Limitations of continuum model

Continuum models of the cell aim at capturing its passive dynamics. In addition to the limitations mentioned above, current models do not yet typically account for active biology: deformations and stresses experienced as a direct consequence of biochemical responses of the cell to mechanical load cannot be predicted by current continuum models. However, by contrasting the predicted purely mechanical cell response to experimental observations, one could isolate phenomena involving active biology, such as cell contraction or migration, from the passive mechanical response of the cell. Alternatively, continuum models might be envisioned that account for active processes through time-dependent properties or residual strains that are linked to biological processes. (See also Chapter 10.)

Another limitation of continuum models stems from lack of description of cytoskeletal fibers. As such, they are not applicable for micromanipulations of the cell with a probe of the same size or smaller than the cytoskeletal mesh ($\sim$0.1–1.0 μm). This includes most AFM experiments. In addition, the continuum models exclude small Brownian motions due to thermal fluctuations of the cytoskeleton, which would correspond to fluctuations of the network nodes in a continuum model and have been shown to play a key role in cell motility (Mogilner and Oster, 1996).

Finally, continuum models have so far employed a limited number of time constants to characterize the cell's behavior. However, cells have recently been shown to exhibit behaviors with power-law rheology implying a continuous spectrum of time scales (Fabry et al., 2001; Desprat et al., 2004, and Chapter 3). Modeling the cell with no intrinsic time constant has successfully captured this behavior (for example, Djordjevic et al., 2003), though this type of model cannot and does not aim at predicting or describing force or strain distribution within the cell. One of the challenges, therefore, to the use of continuum models for the prediction of intracellular stress and strain patterns is to develop cell material models that capture this complex behavior. In the meantime, models involving a finite number of time constants consistent with the time scale of the experimental technique can be used, recognizing their limitations.

Conclusion

Continuum mechanical models have proven useful in exploiting and interpreting results of a number of experimental techniques probing single cells or cell monolayers. They can help identify the stress and strain patterns induced within the cell by experimental perturpations, or the material properties of various cell compartments. In

addition, continuum models enable us to predict the forces experienced within cells *in vivo*, and to then form hypotheses on how cells might sense and transduce forces into behavior such as changes in shape or gene expression.

The time scale of cell stimulation in experiments *in vivo* often requires that we take into account the time-dependent response of the cell, that is, to model it or some of its components as viscous or viscoelastic. Likewise, it is often necessary to model cell compartments with different materials, as their composition gives them very distinct mechanical properties.

Such continuum models have proven useful in the past, and will continue to play a role in cell modeling. As we gain more accurate experimental data on cellular rheology, these results can be incorporated into continuum models of improved accuracy of representation. As such, they are useful "receptacles" of experimental data with the capability to then predict the cellular response to mechanical stimulus, provided one accepts the limitations, and recognizes that they provide little by way of insight into the microstructural basis for macroscopic rheology.

References

Barthes-Biesel, D. 1996. Rheological models of red blood cell mechanics. In Advances in Hemody- namics. How HT, editor. Ed. JAI Press. 31–65.

Bathe, M., A. Shirai, C. M. Doerschuk, and R. D. Kamm. 2002. Neutrophil transit times through pulmonary capillaries: The effects of capillary geometry and fMLP-stimulation. *Biophys. J.*, 83(4):1917–1933.

Charras, G. T., and M. A. Horton. 2002. Determination of cellular strains by combined atomic force microscopy and finite element modeling. *Biophys. J.*, 83(2):858–879.

Charras, G. T., P. P. Lehenkari, and M. A. Horton. 2001. Atomic force microscopy can be used to mechanically stimulate osteoblasts and evaluate cellular strain distributions. *Ultramicroscopy*, 86(1–2):85–95.

Dahl, K. N., Engler, A. J., Pajerowski, J. D. & Discher, D. E. 2005. "Power-law rheology of isolated nuclei with deformation mapping of nuclear substitution." *Biophys. J.*, 89(4):2855–2864.

Desprat, N., A. Richert, J. Simeon, and A. Asnacios. 2004. Creep function of a single living cell. *Biophys. J.*, :biophysj.104.050278.

Discher, D. E., D. H. Boal, and S. K. Boey. 1998. Simulations of the erythrocyte cytoskeleton at large deformation. II. Micropipette aspiration. *Biophys. J.*, 75(3):1584–1597.

Djordjević, V. D., J. Jarić, B. Fabry, J. J. Fredberg, and D. Stamenović. 2003. Fractional derivatives embody essential features of cell rheological behavior. *Ann. Biomed. Eng.*, 31:692–699.

Dong, C., and R. Skalak. 1992. Leukocyte deformability: Finite element modeling of large viscoelas- tic deformation. *J. Theoretical, Biol.*, 158(2):173–193.

Dong, C., R. Skalak, K. L. Sung, G. W. Schmid-Schönbein, and S. Chien. 1988. Passive deformation analysis of human leukocytes. *J. Biomech. Eng.*, 110(1):27–36.

Drury, J. L., and M. Dembo. 2001. Aspiration of human neutrophils: Effects of shear thinning and cortical dissipation. *Biophys. J.*, 81(6):3166–3177.

Evans, E. 1989. Structure and deformation properties of red blood cells: Concepts and quantitative methods. *Methods Enzymol.*, 173:3–35.

Evans, E., and A. Yeung. 1989. Apparent viscosity and cortical tension of blood granulocytes deter- mined by micropipette aspiration. *Biophys. J.*, 56(1):151–160.

Fabry, B., G. Maksym, J. Butler, M. Glogauer, D. Navajas, and J. Fredberg. 2001. Scaling the microrheology of living cells. *Phys. Rev. Lett.*, 87:148102.

Fung, Y. C., S. Q. Liu. 1993. Elementary mechanics of the endothelium of blood vessels. *ASME J. Biomech. Eng.*, 115: 1–12.

Gracheva, M. E., and H. G. Othmer. 2004. A continuum model of motility in ameboid cells. *Bull. of Math. Bio.*, 66(1):167–193.

Guilak, F., J. R. Tedrow, and R. Burgkart. 2000. Viscoelastic properties of the cell nucleus. *Biochem. and Biophy. Res. Comm.*, 269(3):781–786.

Hsiao, J. 2004. Emerin and inherited disease. Masters thesis. Division of Health Science and Technology, Harvard-MIT, Cambridge.

Hwang, W., and R. Waugh. 1997. Energy of dissociation of lipid bilayer from the membrane skeleton of red blood cells. *Biophys. J.*, 72(6):2669–2678.

Karcher, H., J. Lammerding, H. Huang, R. Lee, R. Kamm, and M. Kaazempur-Mofrad. 2003. A three-dimensional viscoelastic model for cell deformation with experimental verification. *Biophys. J.*, 85(5):3336–3349.

Landman, K. 1984. A continuum model for a red blood cell transformation: Sphere to crenated sphere. *J. Theor. Biol.*, 106(3):329–351.

Laurent, V., S. Henon, E. Planus, R. Fodil, M. Balland, D. Isabey, and F. Gallet. 2002. Assessment of mechanical properties of adherent living cells by bead micromanipulation: Comparison of magnetic twisting cytometry vs optical tweezers. *J. Biomech. Eng.*, 124(August):408–421.

Mack, P. J., M. R. Kaazempur-Mofrad, H. Karcher, R. T. Lee, and R. D. Kamm. 2004. Force-induced focal adhesion translocation: Effects of force amplitude and frequency. *Am. J. Physiol. Cell Physiol*:00567.02003.

Mijailovich, S. M., M. Kojic, M. Zivkovic, B. Fabry, and J. J. Fredberg. 2002. A finite element model of cell deformation during magnetic bead twisting. *J. Appl. Physiol.*, 93(4):1429–1436.

Mills, J. P., L. Qie, M. Dao, C. T. Lim, and S. Suresh. 2004. Nonlinear elastic and viscoelastic deformation of the human red blood cell with optical tweezers. *Mech. and Chem. of Biosys.*, 1(3):169–180.

Mogilner, A., and G. Oster. 1996. Cell motility driven by actin polymerization. *Biophys. J.*, 71(6):3030–3045.

Ohayon, J., P. Tracqui, R. Fodil, S. Féréol, V. M. Laurent, E. Planus, and D. Isabey. 2004. Anaylses of nonlinear responses of adherent epithelial cells probed by magnetic bead twisting: A finite-element model based on a homogenization approach. *J. Biomech. Eng.*, 126(6):685–698.

Sato, M., N. Ohshima, and R. M. Nerem. 1996. Viscoelastic properties of cultured porcine aortic endothelial cells exposed to shear stress. *J. Biomech.*, 29(4):461.

Schmid-Schönbein, G. W., and R. Skalak. 1984. Continuum mechanical model of leukocytes during protopod formation. *J. Biomech. Eng.*, 106(1):10–18.

Schmid-Schönbein, G. W., T. Kosawada, R. Skalak, S. Chien. 1995. Membrane model of endothelial cells and leukocytes. A proposal for the origin of cortical stress. *ASME J. Biomech. Eng.*, 117: 171–178.

Theret, D. P., M. J. Levesque, M. Sato, R. M. Nerem, and L. T. Wheeler. 1988. The application of a homogeneous half-space model in the analysis of endothelial cell micropipette measurements. *ASME J. Biomech. Eng.*, 110:190–199.

Tran-Son-Tay, R., D. Needham, A. Yeung, and R. M. Hochmuth. 1991. Time-dependent recovery of passive neutrophils after large deformation. *Biophys. J.*, 60(4):856–866.

Tseng, Y., Lee, J. S., Kole, T. P., Jiang, I. & Wirtz, D. 2004. Micro-organization and viscoelasticity of interphase nucleus revealed by particle nanotracking. *J. Cell Sci.*, 117, 2159–2167.

Yap, B., and R. D. Kamm. 2005. Mechanical deformation of neutrophils into narrow channels induces pseudopod projection and changes in biomechanical properties. *J. Appl. Physiol.*, 98: 1930–1939.

Yeung, A., and E. Evans. 1989. Cortical cell – liquid core model for passive flow of liquid-like spherical cells into micropipettes. *Biophys. J.*, 56:139–149.

Zaman, M. H., R. D. Kamm, P. T., Matsudaira, and D. A. Lauffenburger. 2005. Computational model for cell migration in 3-dimensional matrices. *Biophys. J.*, 89(2):1389–1397.

Zhelev, D., D. Needham, and R. Hochmuth. 1994. Role of the membrane cortex in neutrophil deformation in small pipettes. *Biophys. J.*, 67(2):696–705.